

Irreversible Electroporation in a Swine Lung Model

Damian E. Dupuy · Bassam Aswad ·
Thomas Ng

Received: 26 May 2010 / Accepted: 3 December 2010 / Published online: 30 December 2010
© Springer Science+Business Media, LLC and the Cardiovascular and Interventional Radiological Society of Europe (CIRSE) 2010

Abstract

Purpose This study was designed to evaluate the safety and tissue effects of IRE in a swine lung model.

Methods This study was approved by the institutional animal care committee. Nine anesthetized domestic swine underwent 15 percutaneous irreversible electroporation (IRE) lesion creations (6 with bipolar and 3 with 3–4 monopolar electrodes) under fluoroscopic guidance and with pancuronium neuromuscular blockade and EKG gating. IRE electrodes were placed into the central and middle third of the right mid and lower lobes in all animals. Postprocedure PA and lateral chest radiographs were obtained to evaluate for pneumothorax. Three animals were sacrificed at 2 weeks and six at 4 weeks. Animals underwent high-resolution CT scanning and PA and lateral radiographs 1 h before sacrifice. The treated lungs were removed en bloc, perfused with formalin, and sectioned.

Gross pathologic and microscopic changes after standard hematoxylin and eosin staining were analyzed within the areas of IRE lesion creation.

Results No significant adverse events were identified. CT showed focal areas of spiculated high density ranging in greatest diameter from 1.1–2.2 cm. On gross inspection of the sectioned lung, focal areas of tan discoloration and increased density were palpated in the areas of IRE. Histological analysis revealed focal areas of diffuse alveolar damage with fibrosis and inflammatory infiltration that respected the boundaries of the interlobular septae. No pathological difference could be discerned between the 2- and 4-week time points. The bronchioles and blood vessels within the areas of IRE were intact and did not show signs of tissue injury.

Conclusion IRE creates focal areas of diffuse alveolar damage without creating damage to the bronchioles or blood vessels. Short-term safety in a swine model appears to be satisfactory.

D. E. Dupuy (✉)
Rhode Island Hospital, The Warren Alpert Medical School
of Brown University, 593 Eddy Street, Providence,
RI 02903, USA
e-mail: ddupuy@lifespan.org

B. Aswad
Department of Pathology, Rhode Island Hospital,
The Warren Alpert Medical School of Brown University,
593 Eddy Street, Providence, RI 02903, USA
e-mail: baswad@lifespan.org

T. Ng
Department of Surgery, Rhode Island Hospital,
The Warren Alpert Medical School of Brown University,
593 Eddy Street, Providence, RI 02903, USA
e-mail: tng@usasurg.org

Introduction

Electroporation is a new nonthermal ablative technique that is being investigated for the treatment of solid malignancies. To date, there have been few preclinical studies published for electroporation [1–6]. The technology can be applied in a reversible (RE) or an irreversible manner (IRE). In either technique, high-voltage electrical impulses are delivered to tissue in rapid, short intervals (microseconds). The result is disruption of the lipid bilayer of the cell, which creates small pores that allow molecules to enter and leave the cell; if permanent, this leads to cell dysregulation and death [3]. IRE like thermal ablative techniques is a minimally invasive technique proposed for

controlled elimination of small volumes of tissue. However, IRE kills cells through a nonthermal mediated technique. Thermal ablative techniques are limited in certain anatomic regions due to thermal sinks from larger vessels and potential thermal injury to collateral tissues, such as hollow viscera, airways, nerves, and skin [7]. Lung tumors have been treated with thermal ablation, but collateral injury to central structures as well as prominent central thermal sinks make it less safe and efficacious in the inner third of the lung and mediastinum. To date, IRE has not been evaluated in the lung. If tumors closer to the chest wall, hilum, and mediastinum could be ablated with IRE due to lack of blood flow interference and lack of thermal injury to adjacent healthy tissue, then many patients with thoracic malignancies who are not surgical candidates may benefit [8]. In this study, we evaluated the safety and tissue effects of IRE in a swine lung model.

Materials and Methods

This study was approved by the institutional animal care and use committee. Nine domestic swine (*sus scrofula*) were premedicated with glycopyrrolate (parasympatholytic) (003 mg/kg IM), Telazol (sedative) (Fort Dodge Laboratories, Fort Dodge, IA) (5 mg/kg IM), and xylazine (alpha blockade anesthetic) (2 mg/kg IM), and surgical anesthesia further induced with sodium thiopental (20 mg/kg IV) via an indwelling catheter placed in an auricular vein, as needed to intubate. The animal was then placed on a mechanical ventilator and maintained at a surgical plane of anesthesia with isoflurane (2–4%) in oxygen. A surgical plane of anesthesia was determined by using jaw tone and pedal reflex; anesthesia was increased if response to stimuli was noted. A baseline evoked motor response was obtained with a nerve stimulator (ulnar nerve). The right lateral thoracic wall was sterilely prepared for percutaneous placement of the IRE device. Because the high direct current voltages of the IRE pulses cause muscle contraction, neuromuscular blockade is necessary. Before administering pancuronium (paralytic) (0.2 mg/kg) IV, a small thoracic incision was made at the insertion point of the IRE electrode. ECG, heart rate, respiratory rate, rectal temperature, pulse-oximetry, and end-tidal CO₂ were monitored and documented at least every 15 min. Evoked motor response was monitored during the interval of muscle relaxation and was continued until full muscle function was restored. The muscle relaxation was reversed, if necessary, with a mixture of edrophonium (0.5 mg/kg) and atropine (0.005 mg/kg) IV.

Using a portable C-arm radiographic unit for fluoroscopic guidance the IRE electrode(s) were inserted into

properly sized regions of mid and lower lobes of the right lung. The needle was introduced deep enough into the lung to ensure close contact with the pulmonary hilum without directly puncturing the main stem bronchi or major cardiopulmonary vasculature. The available IRE electrodes (Nanoknife, Angiodynamics, Latham, NY) are bipolar electrodes with a fixed active tip of 2.7 cm or monopolar electrodes with a retractable sheath insulation, which can be changed from 1–4 cm of electrode exposure. Two bipolar IRE lesions were created in six animals with the following parameters (ninety 70 ms pulses at 2700 V) and a monopolar ablation (2 cm electrode exposure) with electrodes spaced 1–2 cm apart (4 electrodes in two animals and 3 electrodes in one animal) was performed in the lower lung of three animals with the following parameters (ninety 70 ms pulses at 1700–3000 V [depending on the distance between electrodes]) using a Nanoknife IRE generator (Angiodynamics, Latham, NY) capable of creating IRE lesions with up to six electrodes with a maximum current delivery of 50 A and 3000 V (Table 1). More specific generator details can be found at the company's website (<http://www.angiodynamics.com/uploads/pdf/03-03-10-03-49-41-NanoKnife%20IFUs.pdf>). At the end of the monopolar IRE treatment, a small 5-mm platinum Hilal microcoil (Cook Medical, Bloomington, IN) was inserted through a 21-gauge spinal needle into the lung adjacent to the IRE electrodes to assist in the identification of the IRE lesion on CT and at gross pathology. To prevent cardiac arrhythmias, cardiac synchronization via EKG gating was performed in all animals with pulses triggered to the refractory period after the R wave. Postprocedure PA and lateral chest radiographs were obtained to evaluate for pneumothorax. Identified pneumothoraces were aspirated using a 5-F Yueh catheter (Cook Medical). Animals underwent pentobarbital euthanasia (100 mg/kg) after being placed under general anesthesia for follow-up imaging. Three animals treated with bipolar IRE electrodes were killed at 2 weeks and the remaining six animals at 4 weeks. Animals underwent high-resolution 64-detector CT scanning (General Electric VCT, GE Medical Systems, Milwaukee, WI) at 0.625-mm increments (5-mm slice reconstruction), pitch of 1.375:1, 120 kV, and 770 mA during suspended respiration and without intravenous contrast immediately before euthanasia. PA and lateral radiographs were obtained 1 h before euthanasia. The treated lungs were removed en bloc, infused with formalin for 24 h, and sectioned. Gross pathologic and microscopic changes after standard hematoxylin and eosin staining were analyzed by a single board-certified pathologist within the areas of IRE lesion creation. Parenchymal abnormalities corresponding to the ablated lobe were measured in two axial dimensions on CT.

Table 1 Treatment parameters for IRE

Swine #	Needle type	Needle #	Spacing range	Voltage range	Pulses	Pulse length (μ s)	Maximum ampere range
1–6	Bipolar	1	Fixed	Fixed 2700	90	70	10–17
7	Monopolar	4	1.5–2.0	2500–3000	90	70	12.7
8	Monopolar	4	1.0–1.1	1700	90	70	5.3–21.8
9	Monopolar	3	1.2–2.0	2500–3000	90	70	6.7–8.9

Results

All nine swine successfully completed IRE treatment without any cardiac arrhythmias. One animal developed a small pneumothorax directly after removal of a bipolar electrode, which was successfully aspirated under fluoroscopic guidance and did not require additional chest tube drainage. Two animals developed malaise and fever 2 and 4 days after IRE, which resolved spontaneously in one and was treated with oral antibiotics in another. One animal, which had four monopolar electrodes placed, developed trace hemoptysis, which resolved within several hours after extubation. Early 1 h after and 2 and 4 weeks after, IRE chest radiographs did not show any pneumothoraces, pleural effusions, or focal abnormalities. CT showed focal areas of ill-defined, spiculated, high-density with an average size of 1.5 cm ranging in greatest diameter from 1.1–2.2 cm (Fig. 1). Bipolar lesions were larger (greatest diameter range 11–22 mm) and more visible on CT compared with the monopolar ablations (greatest diameter range 10–15 mm). At autopsy, two animals had evidence of pleural adhesions (Fig. 2), one of which was the animal that required antibiotics. This animal also had evidence of right lower lobe consolidation, which was not visible on chest radiographs.

On gross inspection of the sectioned lung, focal areas of tan and yellow discoloration and increased density measuring between 0.2 and 2.5 cm were palpated in the areas of IRE. Histological analysis revealed focal areas of diffuse alveolar damage with fibrosis and inflammatory infiltration that respected the boundaries of the interlobular septae (Fig. 3). The bronchioles and blood vessels within the areas of IRE were intact and did not show signs of tissue injury (Fig. 3). Placement of the IRE electrodes in the inner third of the lung was not as successful as planned due to the fact that the needles were placed with single plane fluoroscopy. All of the IRE lesions were in the middle or outer third of the lung. However, arterioles measuring between 0.2 and 1.0 mm and bronchioles measuring between 0.3 and 1.5 mm were within the IR zone. Blood vessel and bronchiolar walls contained mild chronic inflammatory changes and hemosiderin deposition but remained intact with no thrombosis or collapse. The cartilage rings of the

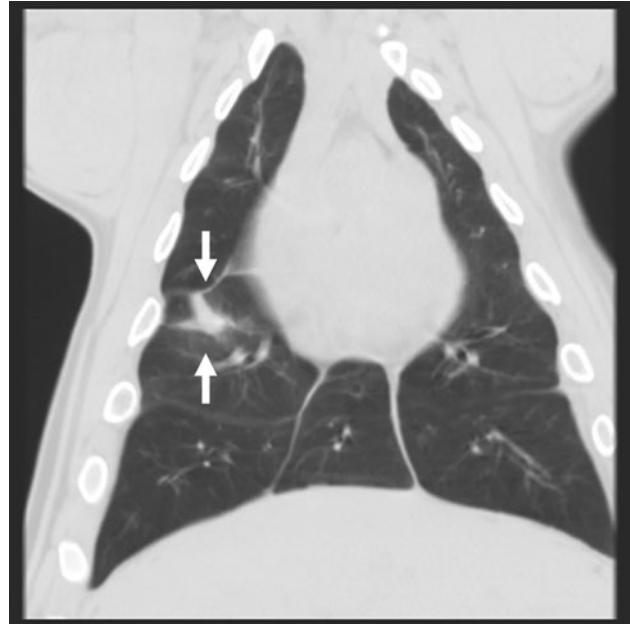


Fig. 1 Coronal reconstructed CT image through the lung of a pig treated with bipolar IRE 2 weeks previously. Spiculated soft-tissue density (arrows) corresponds to the IRE lesion

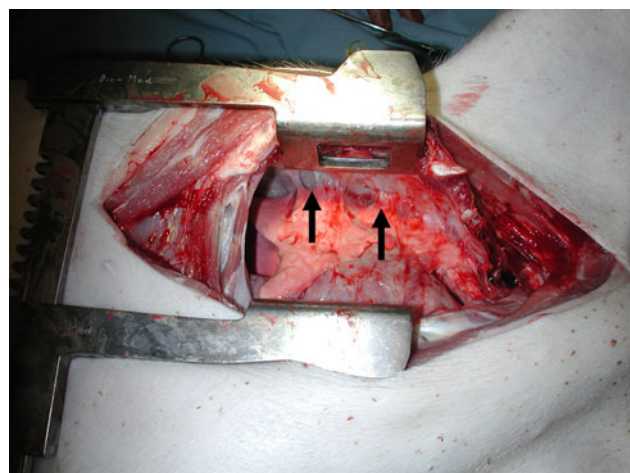


Fig. 2 Photograph of right hemithorax after thoracotomy in a pig treated with bipolar IRE reveals extensive pleural adhesions (arrows). This pig developed postprocedure fevers that required antibiotics. Lobar consolidation was found at autopsy in a lobe separate from the IRE treatment

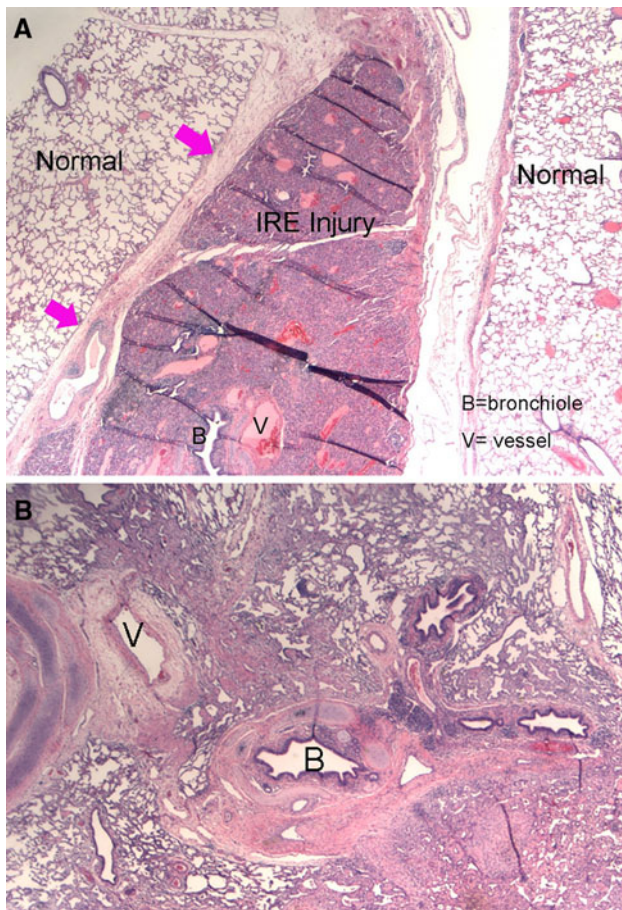


Fig. 3 **A** Bipolar IRE ablation zone 2 weeks after treatment with H&E staining shows the central IRE injury demarcated by the interlobular septae (pink arrows) without evidence of thermal sink effect around the bronchiole or pulmonary artery. **B** High-power magnification of the artery (V) and airway (B) show patency within the IRE lesion

bronchioles remained normal in appearance. On review of the pathology between the 2- and 4-week time points, the healing process could be detected as reactive pneumocytes, focal inspissated material in residual bronchioles and air spaces, metaplastic epithelial cells (e.g., pneumocytes, bronchiolar cells), and hemopexin (breakdown product of hemosiderin).

Discussion

Irreversible electroporation results in tissue necrosis presumably due to apoptotic cell death. Previous reports suggest a narrow transition between the zone of tissue necrosis and healthy tissue. We have shown similar findings in swine lung where the IRE lesion is demarcated by the interlobular septae and the bronchioles and blood vessels within the affected region were not damaged.

Importantly, tissue adjacent to these major vascular structures showed tissue injury, suggesting a potential major advantage over currently available thermal ablation technologies whereby thermal sinks can affect the ablation zone. This tissue healing effects seen in lung is different than what Lee and colleagues observed in liver whereby healing appears more complete [1]. The differences may be related to the less sterile respiratory environment in lung tissue in the swine model compared with the liver. Lee and colleagues showed larger IRE ablation zones averaging 3.4 cm in greatest diameter in swine liver tissue with preservation of blood vessels and bile ducts [1]. The larger ablation zone in their study can be explained by better electrical current conduction in solid tissue compared with aerated lung. In fact in our study the applied current was typically much lower, whereas in liver tissue IRE the current deposition is usually higher. Demarcation of the IRE lesion by the interlobular septae may be due to the underlying healing process or due to a relative insulating effect of the IRE energy by the interlobular septae. Compared with more acute (less than 24 h) IRE, lesions in lung tissue would help to determine which effect is involved. There are no human or animal data in lung tissue for comparison.

Miller et al. performed IRE *in vitro* on human hepatocarcinoma cells [9]. They reported complete cancer cell ablation with the application of 1500 V/cm in three sets of ten pulses of 300 ms. Other investigators have reported success with IRE in cutaneous tumors implanted in mice, dog prostate, and pig liver [10–12]. At the margin of an IRE lesion, surrounding cells may undergo RE. In theory this effect may be used to augment chemotherapy for certain tumors. RE has been used to promote uptake of chemotherapy into tumor cells: electroporation. Allegretti and Panje reported the use of electroporation with intralesional bleomycin for the treatment of 14 patients with head and neck cancers [13]. In this series, six patients had a complete response, six patients had a partial response, and two patients did not respond, for an overall response rate of 86%. They reported no treatment-related deaths and a low procedure-related morbidity.

There are multiple limitations to this study. First, we only studied the 2- and 4-week time points, therefore, earlier and more delayed pathological changes are unknown. Second, we did not use CT guidance to place the electrodes, so our placement was not as central as we would have liked, and the range of distances from the individual monopolar electrode tips was greater than we would have liked. Monopolar tip distances as large as 2.0 cm may have accounted for the smaller lesions seen with the monopolar IRE. Third, lesion visualization can be difficult after fixation, and size measurement can be underestimated due to fixation and lung deflation.

Our study showed relatively small treatment effects in aerated lung, which may make obtaining a margin in human lung tumors difficult. Combining chemotherapy to IRE in human lung tumors in anatomic areas that are too difficult to treat with radiotherapy due to previous radiotherapy or standard thermal ablation techniques may overcome this effect. Future human lung tumor trials looking at the safety and effectiveness of IRE should be performed.

Conclusions

IRE creates focal areas of diffuse alveolar damage without creating damage to the bronchioles or blood vessels. Short-term safety in a swine model appears to be satisfactory. Continued study in human tumors is necessary.

Conflict of interest Damian E. Dupuy, M.D. received grant support from Angiodynamics (Latham, NY) for this study and has received speaking honoraria from Angiodynamics.

References

1. Lee EW, Chen C, Prieto VE, Dry SM, Loh CT, Kee ST (2010) Advanced hepatic ablation technique for creating complete cell death: irreversible electroporation. *Radiology* 255:426–433
2. Esser AT, Smith KC, Gowrishankar TR, Weaver JC (2007) Towards solid tumor treatment by irreversible electroporation: intrinsic redistribution of fields and currents in tissue. *Technol Cancer Res Treat* 6:261–274
3. Davalos RV, Mir IL, Rubinsky B (2005) Tissue ablation with irreversible electroporation. *Ann Biomed Eng* 33:223–231
4. Bertacchini C, Margotti PM, Bergamini E, Lodi A, Ronchetti M, Cadossi R (2007) Design of an irreversible electroporation system for clinical use. *Technol Cancer Res Treat* 6:313–320
5. Edd JF, Davalos RV (2007) Mathematical modeling of irreversible electroporation for treatment planning. *Technol Cancer Res Treat* 6:275–286
6. Rabussay DP, Nanada GS, Goldfarb PM (2002) Enhancing the effectiveness of drug based cancer therapy by electroporation (electropermeabilization). *Technol Cancer Res Treat* 1:71–82
7. Goldberg SN, Dupuy DE (2001) Image-guided radiofrequency tumor ablation: challenges and opportunities part 1. *J Vasc Interv Radiol* 12:1021–1032
8. McTaggart RA, Dupuy DE (2007) Thermal ablation of lung tumors. *Tech Vasc Interv Radiol* 10:102–113
9. Miller L, Leor J, Rubinsky B (2005) Cancer cells ablation with irreversible electroporation. *Technol Cancer Res Treat* 4:699–705
10. Al-Sakere B, Andre F, Bernat C, Connault E, Opolon P et al (2007) Tumor ablation with irreversible electroporation. *PLoS ONE* 2:e1135
11. Onik G, Mikus P, Rubinsky B (2007) Irreversible electroporation: implications for prostate ablation. *Technol Cancer Res Treat* 4:295–300
12. Rubinsky B, Onik G, Mikus P (2007) Irreversible electroporation: a new modality clinical implications. *Technol Cancer Res Treat* 6:37–48
13. Allegretti JP, Panje WR (2001) Electroporation therapy for head and neck cancer including carotid artery involvement. *Laryngoscope* 111:52–56